LES of oscillating boundary layers under surface cooling

Mario J. Juha, Andrés E. Tejada-Martínez*†, and Jie Zhang

Department of Civil and Environmental Engineering, University of South Florida, USA.

*Presenting author: aetejada@usf.edu
†Corresponding author

Abstract

Large-eddy simulation (LES) of open channel flow driven by an oscillating pressure gradient with zero surface shear stress was performed. The flow is representative of an oscillating tidal boundary layer. Under neutrally stratified conditions, during certain phases of the oscillating pressure gradient corresponding, for example, to peak tide, the flow develops secondary structures, characterized by coherent, full-depth, streamwise-elongated counter-rotating cells. These structures are similar to the classical Couette cells found in Couette flow driven by parallel no-slip plates moving in opposite direction. A constant cooling flux at the surface with an adiabatic bottom wall leads to more intense and coherent streamwise-elongated cells characterized by greater crosswind width, which we term *convective supercells*. The signature of the convective supercells is observed even during times when the oscillating mean flow is decelerating, unlike in cases without surface cooling. Investigation of these coherent structures (with and without surface cooling) is deemed important due to their strong influence on vertical mixing and their potential role in determining the wake behind tidal turbines.

Keywords: Large-eddy simulation, oscillating boundary layer flow, tidal flow, surface cooling, convective supercell, vertical mixing of momentum

Introduction

Large-eddy simulation (LES) of neutrally stratified open channel flows driven with either a constant [1] or oscillating [2] pressure gradient have revealed the presence of secondary, coherent, streamwise-elongated roll cells occupying the full-depth of the water column. These cells, sketched in Figure 1, are similar nature to the well-known Couette cells occurring in channel flow driven by no-slip plates moving in opposite direction [4]. Furthermore, in [1], application of a surface cooling flux to the initially neutrally stratified open channel flow driven by constant pressure gradient led to an unstably stratified flow characterized by wider, intensified streamwise-elongated roll cells. The latter were termed *convective supercells* due to their greater intensity and cross-stream size resulting in greater vertical mixing (e.g. of momentum) throughout the water column.

The goal of the present work is to re-visit open channel flow with an oscillating pressure gradient and to apply, for the first time, a surface cooling flux in order to understand its effect on the structure of the cells throughout the pressure gradient cycle. The pressure gradient is chosen so as to drive an oscillating boundary layer flow with period characteristic of tidal boundary layers. Results will be analyzed via visualizations of the coherent cells revealed by the averaging of instantaneous velocity fluctuations over the streamwise direction (x_1). Additional analysis is presented in terms of the instantaneous streamwise velocity averaged over x_1 and x_2 (the cross-stream direction) at various instances during the tidal cycle in order to understand the vertical mixing of momentum induced by the cells. More in-depth analysis of the flows, for example in terms of their turbulent structure as revealed through Lumley invariant maps [5] at different phases of the tide, will be reserved for a more in-depth journal article.

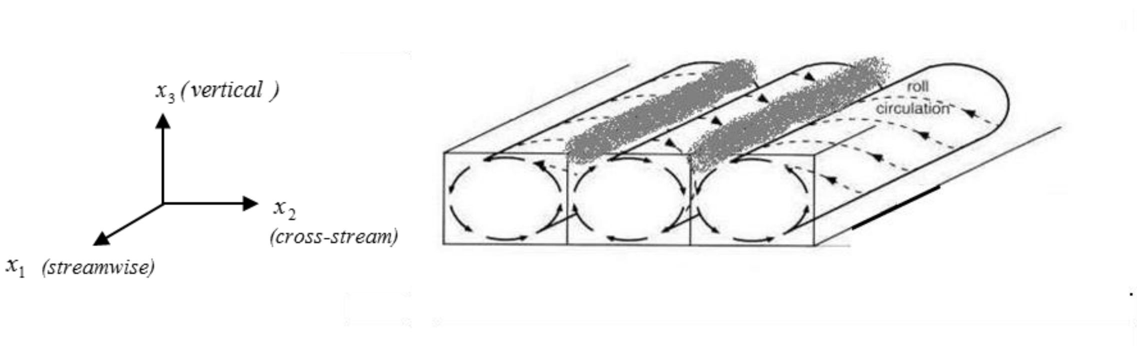

Figure 1. Sketch of streamwise-elongated counter-rotating cells occurring secondary to the mean flow in open channel flow driven by a pressure gradient. In the field such roll cells, characterizing boundary layer flow, could potentially lead to accumulation of lines of floating material along the surface convergence of the cells, as depicted above, similar to the action of Langmuir circulations [3].

In addition to enhancing vertical mixing of momentum and scalars, the previously discussed coherent structures (with and without surface cooling) could potentially have a strong impact on the wake behind a tidal turbine. From a computational engineering analysis perspective, the modeling of the tidal flow and the turbulent wake generated by the turbine are equally important. The most sophisticated simulations of turbines without an accurate model of the tidal flow become as limited as much simpler turbine models. In a similar fashion to wind energy, wake meandering is caused by the large eddies of the ambient flow, such as the coherent cells studied here. Therefore, an accurate model of these large eddies is the most accurate way to capture wake meandering [6] and should be pursued in the future.

Governing LES equations

The spatially filtered or LES equations consisting of conservation of momentum, continuity and temperature (scalar) transport are given by Eqns. (1)-(3), respectively, as

$$\frac{\partial \bar{u}_i}{\partial t} + \frac{\partial \bar{u}_i \bar{u}_j}{\partial x_j} = -\frac{\partial \bar{p}}{\partial x_i} + \frac{1}{Re_\tau}\frac{\partial^2 \bar{u}_i}{\partial x_j^2} + \frac{\partial \tau_{ij}^{SGS}}{\partial x_j} + Ra_\tau \bar{\theta}\delta_{i3} + \frac{1}{Ro}\left(\frac{U_O^{max}}{u_\tau^{max}}\right)^2 \cos\left(\frac{1}{Ro}\frac{U_O^{max}}{u_\tau^{max}} t\right)\delta_{i1} \quad (1)$$

$$\frac{\partial \bar{u}_i}{\partial x_i} = 0 \quad (2)$$

$$\frac{\partial \bar{\theta}}{\partial t} + \frac{\partial \bar{\theta}\bar{u}_j}{\partial x_j} = \frac{1}{PrRe_\tau}\frac{\partial^2 \bar{\theta}}{\partial x_j^2} + \frac{\partial \lambda_j^{SGS}}{\partial x_j} \quad (3)$$

In these equations, an over-bar denotes a filtered quantity with $\bar{u}_i$, $\bar{p}$ and $\bar{\theta}$ being the filtered velocity, pressure and temperature, respectively. Time and the spatial coordinates in the streamwise, cross-stream and vertical (depth) directions are given by t, x_1, x_2 and x_3, respectively. The third term on the right hand side of Eqn. (1) is comprised of the LES subgrid-scale (SGS) stress, τ_{ij}^{SGS}, modeled here through a dynamic Smagorinsky model (not shown). The fourth term on the right side of Eqn. (1) represents buoyancy acting on the vertical (x_3) momentum equation and the fifth term is an oscillating pressure gradient (or tidal body force) driving the mean flow in the positive or negative x_1 direction. Note that the body force has been defined to drive a maximum dimensional free stream velocity U_O^{max} following the formulation in [2]. The second term on the right hand side of Eqn. (3) contains the SGS scalar flux λ_j^{SGS} modeled in terms of an eddy diffusivity taken as the dynamic Smagorinsky eddy viscosity (not shown) divided by turbulent Prandtl number, the latter set to 1.

Equations (1)-(3) have been made dimensionless with characteristic velocity and length scales given by the maximum wall friction velocity u_τ^{max} and water column half-depth δ, respectively. Temperature has been non-dimensionalized via the magnitude of the vertical temperature gradient at the surface (i.e. at the top of the water column) defined as Q/k where Q is the surface cooling flux and k is the thermal conductivity. Specifically, the characteristic temperature is taken as $Q\delta/k$.

Non-dimensionalization of the governing equations gives rise to the Reynolds, Rayleigh, Rossby and molecular Prandtl numbers defined as $Re_\tau = u_\tau^{max}\,\delta/\nu$, $Ra_\tau = g\beta\delta^2 Q/({u_\tau^{max}}^2 k)$, $Ro = U_O^{max}/(\delta\,\omega)$ and $Pr = \nu/\kappa$, respectively. In these definitions, ν is kinematic viscosity, β is the coefficient of thermal expansion, ω is tidal frequency and κ is thermal diffusivity in water. Note that the Rayleigh number is indicative of the strength of surface buoyancy forcing relative to wall shear forcing. The Rossby number is proportional to the oscillatory boundary layer thickness relative to the water column half-depth.

Computational setup

Figure 2 shows a sketch of the computational domain for the LES. The domain consists of an open channel with periodic boundary conditions in the streamwise (x_1) and cross-stream (x_2) (i.e. the horizontal) directions. The top surface of the channel is open with imposed shear-free and cooling boundary conditions. The bottom of the channel consists of an adiabatic wall. The channel is $4\pi\delta$ long in the streamwise direction and $8\pi\delta/3$ wide in the cross-stream direction. The latter length was chosen so as to resolve one pair of convective supercells, as sketched in Figure (1), in simulations with surface cooling.

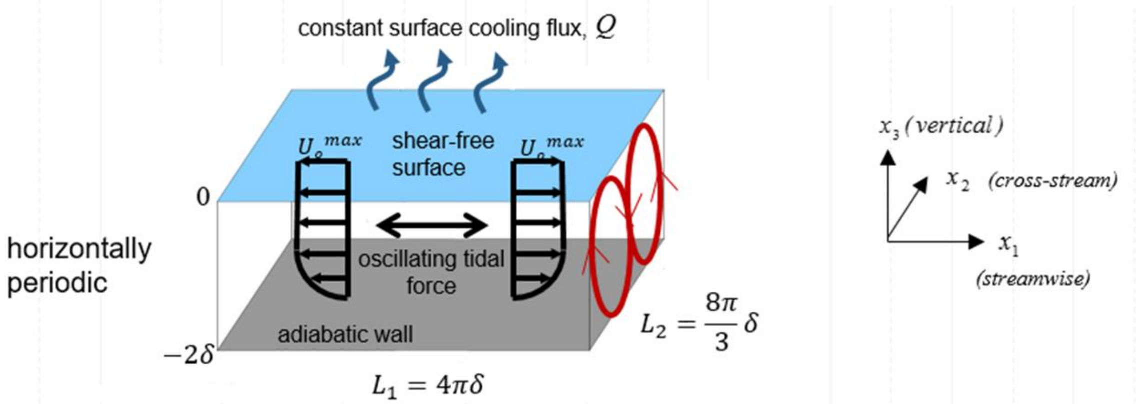

Figure 2. Sketch of computational domain displaying boundary conditions, the driving oscillating pressure gradient (or tidal force), the resulting mean velocity vectors and the secondary general circulation associated with convective supercells (red circles).

The pressure gradient (tidal force) frequency has been set such that the Rossby number Ro is equal to 878, following the tidal boundary layer simulations in [1]. This Rossby number value was obtained for a water column 10 meters deep (corresponding to δ = 5 m) with U_0^{max} = 0.5 m s^{-1} and frequency ω corresponding to a tidal period of approximately 12.5 hr. Furthermore, in the oscillating pressure gradient on the right hand side of Eqn. (1), the ratio U_0^{max}/u_τ^{max} has been set equal to the corresponding value obtained in a preliminary open channel simulation with constant pressure gradient prescribed such that Reynolds number Re_τ is equal to 395. Simulations with either Raleigh number Ra_τ set to 0 or 250 were performed. Ra_τ = 0 corresponds to zero surface heat flux Q and Ra_τ = 250 corresponds to Q of about 200 Watts m^{-2}. Molecular Prandtl number Pr was set to 1.

The computational domain was discretized with 32 uniformly spaced points in the streamwise, 64 uniformly spaced points in the cross-stream direction and 65 uniformly spaced points in the vertical direction. The vertical distribution of grid points is such that the viscous and buffer wall sublayers are not resolved, and thus a wall model was used. The numerical discretization consisted of the finite volume method along with time integration implemented in the popular open source code openFOAM [7].

Results

First we take a look at results for the flow with Ra_τ = 0. In Figure 3, on the panel on the right we can see the instantaneous velocity profiles averaged over the streamwise and crosswind directions at various instances during the tidal cycle. Velocity profiles in the LES are shown in solid and log-law fits of the LES solution through the first 6 grid points from the wall are shown with dots. Throughout the instances during the tidal cycle being shown, it is seen that the LES velocity is well-approximated by a log law.

On the panels on the left, in Figure 3, we can see instantaneous velocity fluctuations averaged over the streamwise direction. On the panels on the left the vertical axis covers the vertical extent of the water column and the horizontal axis covers the crosswind extent of the domain.

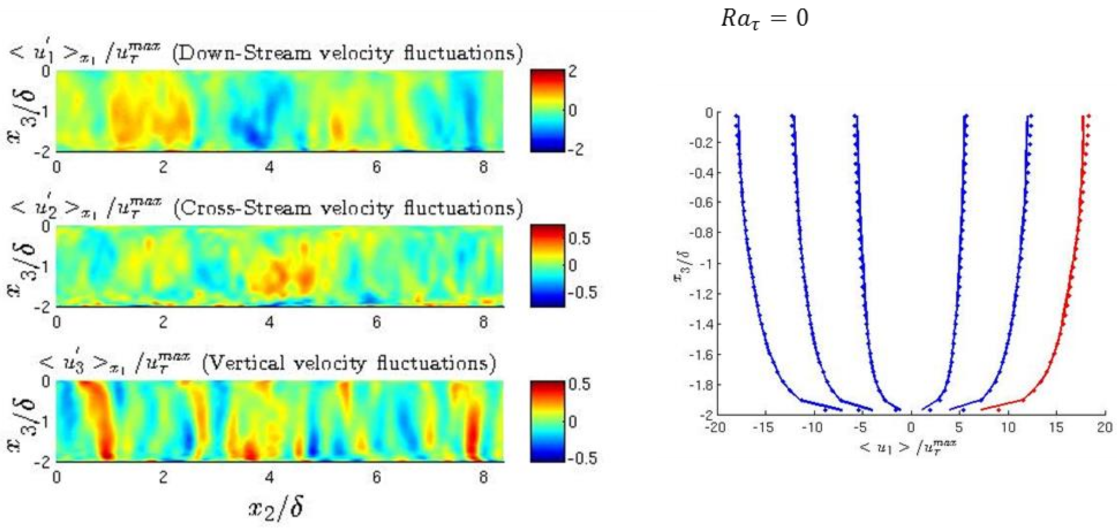

Figure 3. Panel on right: Depth profiles of instantaneous streamwise velocity averaged over horizontal directions (panel on right) in flow with Ra_τ = 0. Panels on left: Instantaneous, streamwise-averaged velocity fluctuations at the time corresponding to the velocity profile colored in red on the panel on the right.

The instantaneous snapshot of the velocity fluctuations seen on the left corresponds to the peak tide mean velocity profile shown in red on the panel on the right. At peak tide, the flow with Ra_{τ} = 0 is characterized by Couette-like cellular structures spanning the entire depth of the water column, as described earlier. For example, full-depth regions of negative and positive vertical velocity fluctuations can be seen on the lower panel on the left. The full-depth regions of negative vertical velocity fluctuations correspond to the downwelling limbs of the cells being resolved. These dowelling limbs of the cells generally coincide with a full-depth region of positive downwind velocity fluctuations as seen on the top panel on the left.

As the tidal current decelerates, the structures previously described become weaker, which can be seen in Figures 4 and 5. Furthermore, note that during the acceleration stage the cells are not as coherent (i.e. visible) as those during the deceleration stage. These less coherent cells are not shown here for brevity.

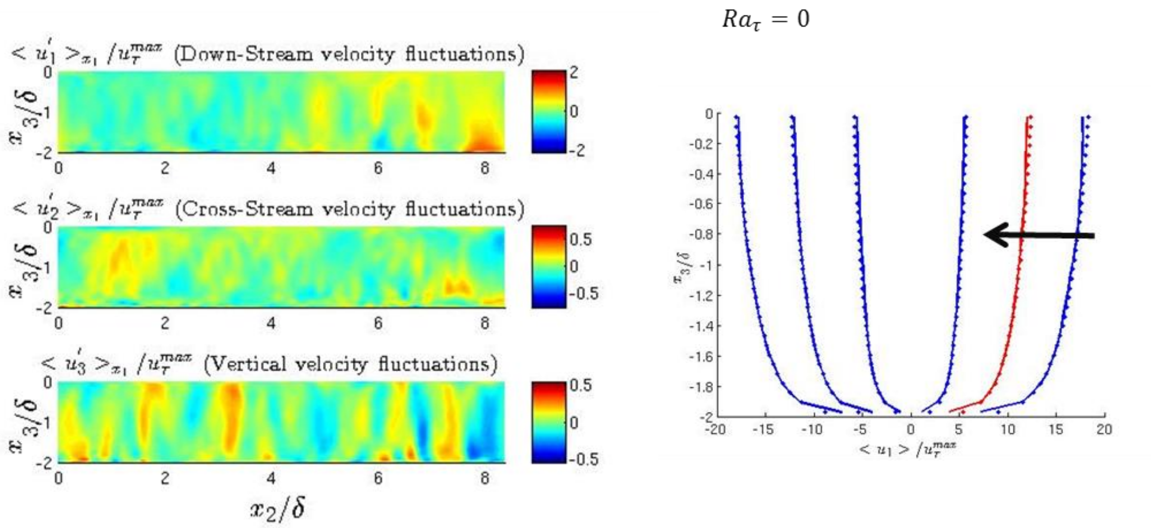

Figure 4. Same as caption of Figure 3 but for flow during deceleration stage.

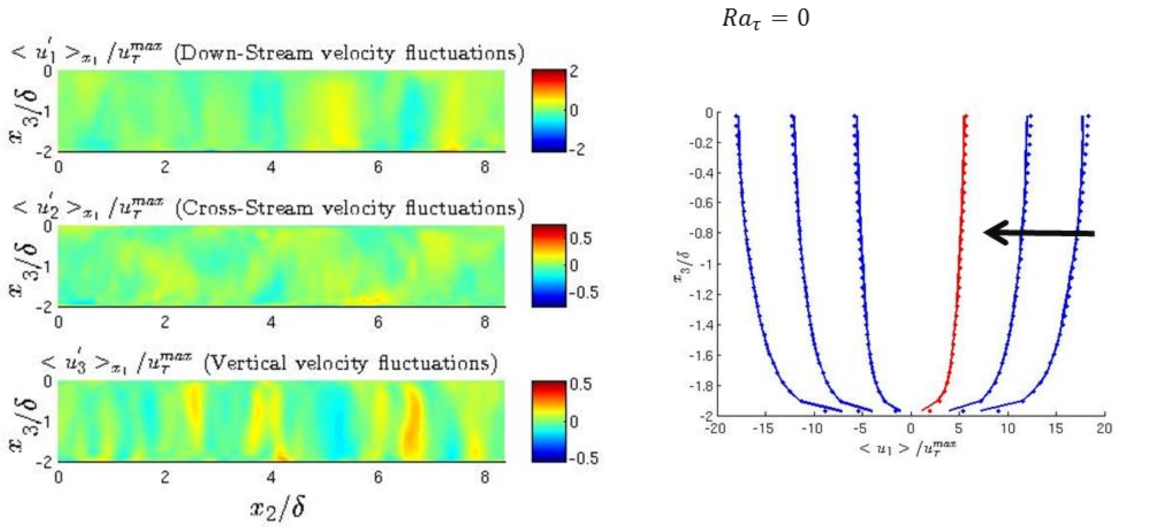

Figure 5. Same as caption of Figure 3 but for flow during deceleration stage.

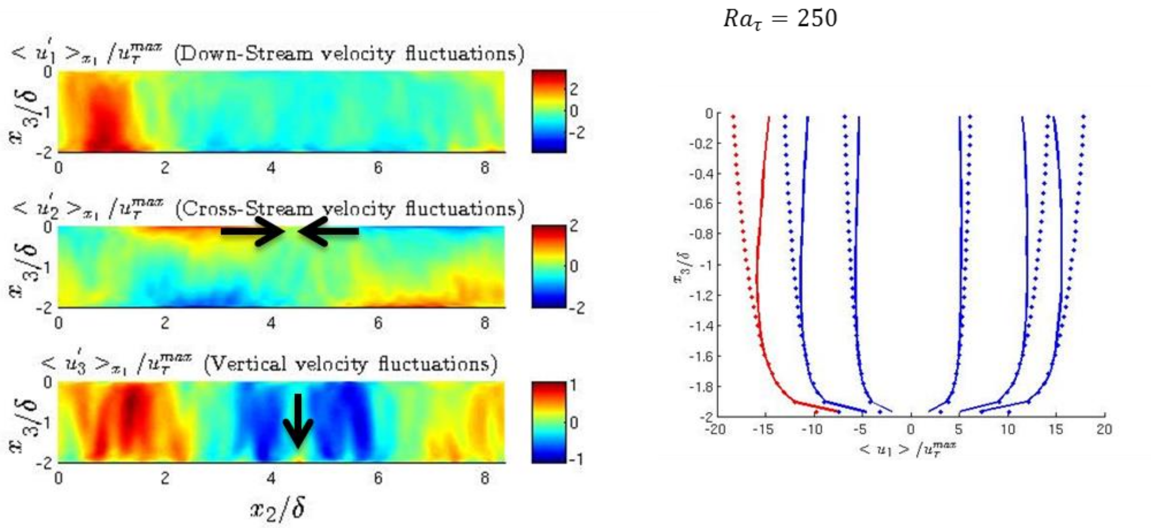

Figure 6. Panel on right: Depth profiles of instantaneous streamwise velocity averaged over horizontal directions (panel on right) in flow with Ra_τ = 250. Panels on left: Instantaneous, streamwise-averaged velocity fluctuations at the time corresponding to the velocity profile colored in red on the panel on the right.

Next we explore the flow with Ra_τ = 250. Throughout the cycle, the mean velocity is well homogenized and thus deviates from the classical log-law as seen on the panel on the right in Figure 6. Recall that the log-law is given by the dots and the LES velocity is given by the solid lines. In Figure 6, on the panels on the left we now see the presence of one cell, more coherent and wider (over the crosswind direction) than the cells described earlier with Ra_τ = 0. We term this cell as a *convective supercell*, due to its greater intensity.

The surface convergence of the convective supercell resolved is indicated by the black arrows appearing on the middle left panel in Figure 6. These arrows follow the orientation of the partially averaged crosswind velocity fluctuation. The surface convergence of the supercell leads into the full-depth downwelling limb of the cell characterized by negative vertical velocity fluctuation shown in the lower panel on the left indicated by the downward pointing black arrow. The increase in strength of the cellular structure resolved with surface cooling is

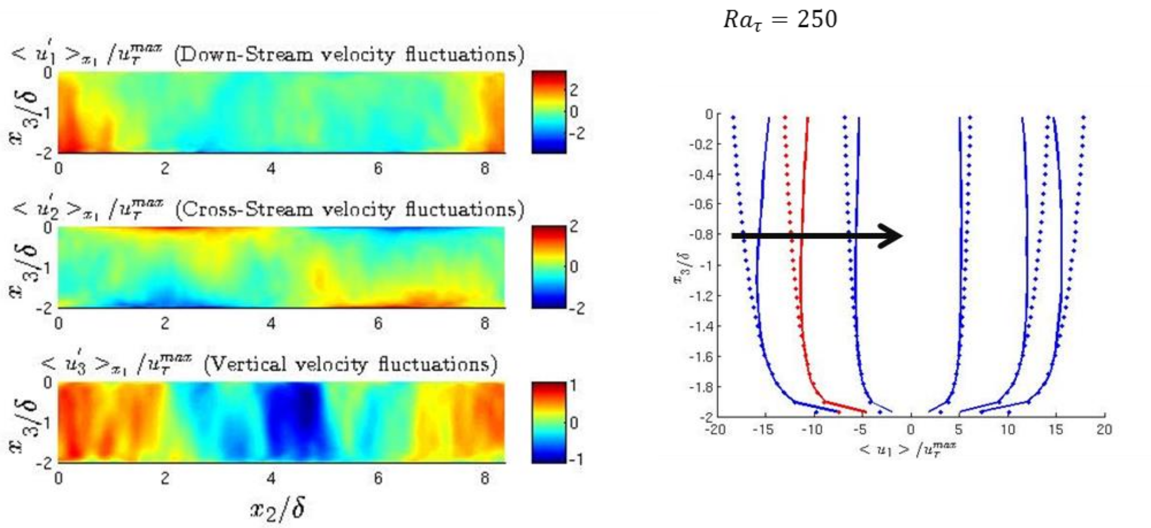

Figure 7. Same as caption of Figure 6 but for flow during deceleration stage.

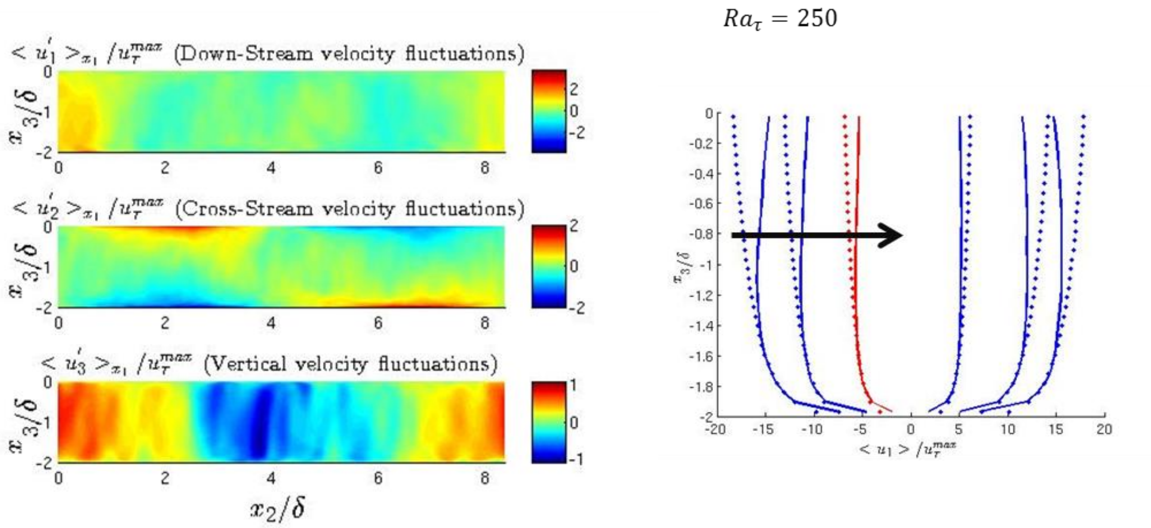

Figure 8. Same as caption of Figure 6 but for flow during deceleration stage.

responsible for the greater homogenization of the velocity profiles shown on the right panel of Figure 6 (i.e. greater vertical mixing of momentum), with respect to the velocity profiles for the flow without surface cooling in Figure 5.

In Figures 7 and 8, it can be seen that despite losing some strength as the flow decelerates, the convective supercell resolved remains visible and significantly serves to increase vertical mixing of momentum throughout the entire tidal cycle, relative to the flow without surface cooling.

As the flow transitions from deceleration to acceleration, remnants of the convective supercell can be observed in Figure 9, regaining strength as the flow accelerates back towards peak tide (Figure 10).

Conclusions

Unstratified open channel flow driven by an oscillating pressure gradient tidal (body) force and zero surface heat flux was shown to be characterized by weakly coherent streamwise-elongated counter-rotating cells occupying or engulfing the bulk of the water column. Surface

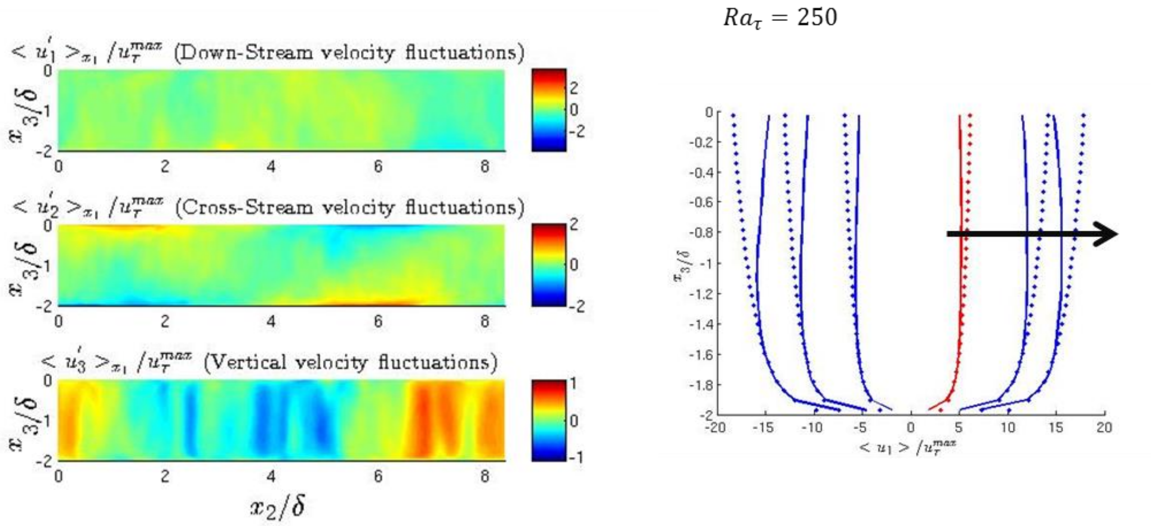

Figure 9. Same as caption of Figure 6 but for flow during acceleration stage.

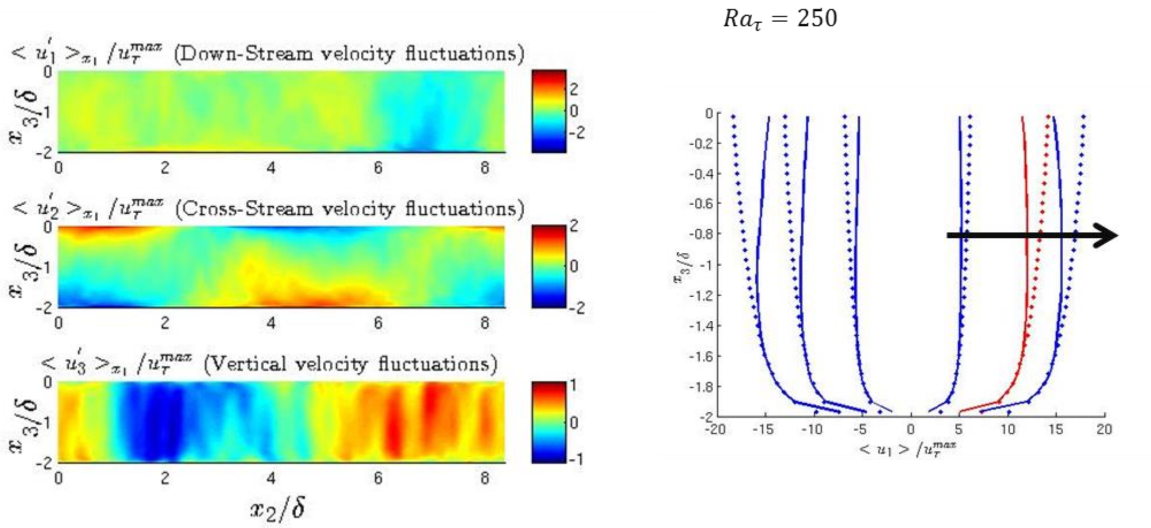

Figure 10. Same as caption of Figure 6 but for flow during acceleration state.

cooling with a heat flux of about 200 Watts m^{-2} led to convective supercells characterized by greater crosswind width and greater intensity and coherency. These cells are able to homogenize the depth profile of the mean velocity, causing deviation from the classical log-law velocity profile, throughout the entire tidal cycle. Although it was not shown here, the surface cooling and associated convective supercells are able to alter the turbulence structure throughout the water column. For example in flow without surface cooling, the middle of the water column is characterized by shear-dominated turbulence throughout the tidal cycle. In the flow with surface cooling of about 200 Watts m^{-2}, the stronger cells are able to induce higher vertical velocity fluctuations in the middle of the water column leading towards an isotropic turbulence structure as the flow transitions from deceleration to acceleration. In a future journal article we will explore the changing turbulence structure throughout the tidal cycle with and without surface cooling with the aid of Lumley invariant maps [5] in addition to the effects of Reynolds, Rossby and Raleigh number on the structure of the convective supercells and the turbulence.

References

[1] Walker, R, Tejada-Martínez, A.E., Martinat, G. and Grosh, C.E. (2015) Large-eddy simulation of open chanel flow with surface cooling, *International Journal of Heat and Fluid Flow* **50**, 209 – 224.

[2] Li. M, Sanford, L., and Chao, S.Y (2005) Effects of time dependence in unstratified tidal boundary layers: results from large eddy simulations, *Estuarine Coastal and Shelf Science* **62**, 193 – 204.

[3] Thorpe, S.A. (2004) Langmuir Circulation, *Annu. Rev. Fluid Mech* **36**, 55 – 79.

[4] Papavassiliou, D.V., Hanratty, T.J., (1997) Interpretation of large-scale structures observed in a turbulent plane Couette flow. *Int. J. Heat Fluid Flow* **18**, 55–69.

[5] Pope, S.B. (2000) Turbulent Flows. *Cambridge University Press*.

[6] Fernandez, A. Personal communication.

[7] openFOAM User Manual.